

## Leidenfrost drops

Anne-Laure Bianco Christophe Clanet David Quéré

Citation: *Physics of Fluids* **15**, 1632 (2003); doi: 10.1063/1.1572161

View online: <http://dx.doi.org/10.1063/1.1572161>

View Table of Contents: <http://aip.scitation.org/toc/phf/15/6>

Published by the [American Institute of Physics](#)

---

### Articles you may be interested in

[Two dimensional Leidenfrost droplets in a Hele-Shaw cell](#)

*Physics of Fluids* **26**, 032103032103 (2014); 10.1063/1.4867163

[The many faces of a Leidenfrost drop](#)

*Physics of Fluids* **27**, 091109091109 (2015); 10.1063/1.4930913

[Increasing Leidenfrost point using micro-nano hierarchical surface structures](#)

*Physics of Fluids* **103**, 201601201601 (2013); 10.1063/1.4828673

[Dynamic interactions of Leidenfrost droplets on liquid metal surface](#)

*Physics of Fluids* **109**, 121904121904 (2016); 10.1063/1.4963157

---

The image is a composite graphic. On the left, a green banner contains the text "Searching? Trust CiSE." in white and black. In the center, a screenshot of a Google Scholar search for "python in scientific computing" is shown. The search results list several articles, with the top one being "Python for scientific computing" by T. E. Oliphant, published in *Computing in Science & Engineering*, 2007. A green circle highlights the title of this article. To the right of the search results is a book cover for "Computing in Science & Engineering" featuring a colorful illustration of a city and a globe. On the far right, a green banner contains the text "It's peer-reviewed and appears in the IEEE Xplore and AIP library packages." in white.

## Leidenfrost drops

Anne-Laure Bianco

Laboratoire de Physique de la Matière Condensée, UMR 7125 du CNRS, Collège de France, 75231 Paris Cedex 05, France

Christophe Clanet

Institut de Recherche sur les Phénomènes Hors Équilibre, UMR 6594 du CNRS, BP 146, 13384 Marseille Cedex, France

David Quéré

Laboratoire de Physique de la Matière Condensée, UMR 7125 du CNRS, Collège de France, 75231 Paris Cedex 05, France

(Received 30 September 2002; accepted 6 March 2003; published 5 May 2003)

A Leidenfrost drop forms when a volatile liquid is brought in contact with a very hot solid. Then, a vapor film comes in between the solid and the drop, giving to the latter the appearance of a liquid pearl. After a brief description of the shape of a Leidenfrost drop, we show that its size cannot exceed a certain value. Then, we describe the characteristics of the vapor layer on which it floats. We show how it is related to the drop size, and how both vary with time, as evaporation takes place. We finally deduce scaling laws for the lifetime of these drops. © 2003 American Institute of Physics. [DOI: 10.1063/1.1572161]

### I. INTRODUCTION

When a drop of liquid is deposited on a hot solid, of temperature around the boiling temperature of the liquid, the drop boils and quickly vanishes. But if the solid temperature is much higher than the boiling point, the drop is not anymore in contact with the solid, but levitates above its own vapor. Because of the insulating properties of the film, the evaporation is rather slow: a millimetric droplet of water on a metallic surface at 200 °C is observed to float for more than a whole minute. In addition, the absence of contact between the liquid and the solid prevents the nucleation of bubbles, so that the drop does not boil but just quietly evaporates. Such floating drops are called *Leidenfrost drops*, after the name of the German physician who first reported the phenomenon around 1750.<sup>1</sup>

As an example, we display in Fig. 1 the lifetime  $\tau$  of a water drop (radius  $R=1$  mm) deposited on a duralumin plate, as a function of the plate temperature  $T$ . Below 100 °C,  $\tau$  decreases to reach typically 200 ms at 100 °C. At this point, the drop is boiling at once after touching the surface. When heating the plate between 100 and 150 °C, the droplet lifetime dramatically increases, typically by a factor 500, which can be associated with the formation of an insulating vapor layer below the drop. This sharp maximum defines the Leidenfrost temperature.<sup>2,3</sup> At larger temperatures,  $\tau$  slowly decreases, passing from 100 s at 150 °C to 40 s at 350 °C.

The existence and the characterization of the Leidenfrost temperature has been widely investigated.<sup>2-4</sup> It depends on the solid roughness,<sup>5</sup> on the purity of the liquid<sup>6</sup> (which can also affect the lifetime of the drop<sup>7</sup>), and even on the way the liquid is deposited.<sup>8</sup> We focus here on other aspects of the Leidenfrost phenomenon, such as the shape of the drops, their ability to evaporate, and the characteristics of the vapor layer.

### II. DROPS SHAPES AND STABILITY

These levitating drops can be considered as nonwetting. We call *contact* the region where the drop interface is parallel to the solid surface. If the drop radius  $R$  is smaller than the capillary length  $a$  ( $a = \sqrt{\gamma/\rho g}$ , denoting the liquid surface tension and density as  $\gamma$  and  $\rho$ ), the drop is nearly spherical, except at the bottom where it is flattened. In this limit, Mahadevan and Pomeau showed that the size  $\lambda$  of the contact is given by a balance between gravity and surface tension.<sup>9</sup> Denoting  $\delta$  as the lowering of the center of mass, this balance can dimensionally be written:  $\gamma\delta \sim \rho g R^3$ . Together with the geometric Hertz relation  $\lambda \sim \sqrt{\delta R}$ , this yields<sup>9</sup>

$$\lambda \sim R^2/a. \quad (1)$$

This relation was checked experimentally with nonwetting liquid marbles.<sup>10</sup> Drops larger than the capillary length form

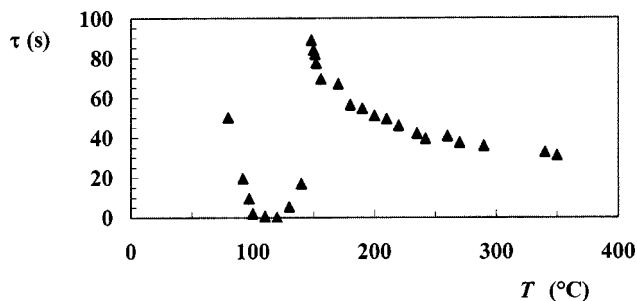


FIG. 1. Lifetime  $\tau$  of a millimetric water droplet of radius  $R=1$  mm, as a function of the temperature  $T$  of the Duralumin plate on which it is deposited.



FIG. 2. Large water droplet deposited on a silicon surface at 200 °C.

puddles flattened by gravity, as it can be observed in Fig. 2, and the contact becomes of the order of the puddle radius ( $\lambda \sim R$ ).

The thickness  $h$  of this puddle is given by balancing the surface tension ( $2\gamma$ , per unit length, taking into account the upper and the lower interface) with the hydrostatic force ( $\rho gh^2/2$ , also written per unit length). This yields

$$h = 2a. \quad (2)$$

The temperature inside the water drop was measured and found to be constant and equal to  $99 \pm 1$  °C. This implies a density  $\rho = 960$  kg/m<sup>3</sup> and a surface tension  $\gamma = 59$  mN/m, and thus a capillary length  $a = 2.5$  mm. For Leidenfrost puddles such as in Fig. 2 or larger, we measured  $h = 5.1$  mm, in good agreement with Eq. (2).

Up to now, the shape of these static drops was found to be characteristic of a situation of nonwetting, close to what can be obtained on superhydrophobic solids. But as an original property, it is observed that the radius  $R$  (and thus the volume  $2\pi R^2 a$ ) of a Leidenfrost drop is bounded, by a value of the order of 1 cm (corresponding to about 1 cm<sup>3</sup> for the volume). If it is larger, a bubble of vapor (or possibly several ones, for very large puddles) rises at the center of the drop and bursts when reaching the upper interface, as reported in Fig. 3.

We interpret this effect as a Rayleigh–Taylor instability<sup>11</sup> of the lower interface. The vapor film tends to rise because of Archimedes' thrust, but this implies a deformation of the lower interface, which the surface tension opposes. Thus, we expect the maximum size of the drop to scale as  $a$ , the capillary length. Classically,<sup>12</sup> the instability threshold can be determined by looking at the evolution of a small sinusoidal perturbation of the lower interface

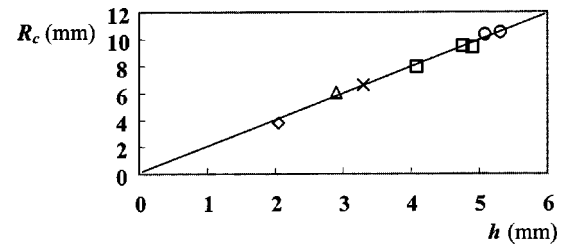


FIG. 4. Largest possible radius  $R_c$  of a Leidenfrost puddle without bubbling, as a function of its height  $h$ . The data are obtained with different fluids [( $\diamond$ ) liquid nitrogen, ( $\triangle$ ) acetone, ( $\times$ ) ethanol, ( $\square$ ) water–ethanol mixtures of various compositions, ( $\circ$ ) water] deposited on a duralumin plate at  $T = 300$  °C. For drops of radius  $R$  larger than  $R_c$ , bubbles such as photographed in Fig. 3 are observed.

$z = \epsilon(1 + \cos kr)$ , with  $\epsilon k \ll 1$  and  $r$  the radial coordinate. The smallest cost in surface energy being achieved for a single bump centered in  $r=0$ , we choose a wave vector  $k = \pi/R$ . Considering capillary and gravitational effects, the difference of pressure  $\Delta P$  between the center and the edge of the drop for two points  $A$  and  $B$  at the same level is  $\Delta P = P_A - P_B = 2\rho g \epsilon [1 - 3(ak)^2/2]$ . The perturbation increases for positive values of  $\Delta P$  and is stabilized for negative ones. The threshold of the instability is thus for  $\Delta P = 0$ , which leads to a critical radius  $R_c = 3.84a$ . Using Eq. (2), we can express this quantity as a function of the puddle height:

$$R_c = 1.92h. \quad (3)$$

Figure 4 shows the largest radius  $R_c$  observed without bubbles as a function of the puddle height, also measured. Different liquids were used in order to vary the capillary length, and thus the height. In particular, the thinner puddles were obtained with liquid nitrogen and oxygen. The variation is indeed linear, and the slope found to be 2, in close agreement with Eq. (3).

### III. THE VAPOR LAYER: STATIONARY STATES

We now investigate the characteristics of the vapor layer supporting the drop. In order to measure its thickness, we used the diffraction of a He–Ne laser beam by the slot made by the interval between the liquid and the solid (Fig. 5). We recorded the diffraction pattern (the distance  $X$  between two maxima is about 1 cm on the screen and three to ten maxima can be observed), and thus could deduce the film thickness  $e$ , which was found to be in the range 10–100  $\mu\text{m}$ .

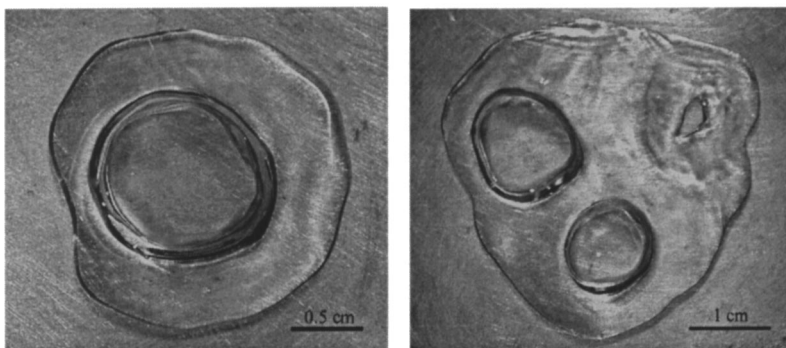


FIG. 3. Large puddles of water on a slightly concave Duralumin plate at 300 °C, seen from above. According to the puddle size, one or several bubbles rise and burst at the upper surface. The bars respectively indicate 0.5 and 1 cm.

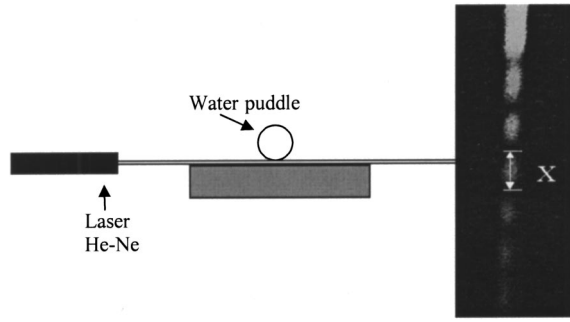


FIG. 5. Experimental setup to measure the thickness of the vapor layer. The photograph on the right shows a typical diffraction pattern, from which the thickness of the vapor film can be deduced.

Since a Leidenfrost drop evaporates, the film thickness is likely to vary with time. We first tried to characterize stationary states. Thus, we looked at the situation where the drop was constantly fed with the liquid, at a prescribed rate (Fig. 6).

In such an experiment, fixing the feeding rate determines the drop radius: the higher the rate, the larger the drop (and above a threshold in rate, we find again the instability described in Sec. II). Moreover, this experiment provides a direct measurement of the evaporating rate, for a given drop radius.

For each rate, we measured the film thickness  $e$ , and observed that it was indeed constant as a function of time. But it does vary with the drop radius, as displayed in Fig. 7. The error bars in Fig. 7 are small (of the order of the symbol size) because each point is an average on 30–50 experiments.

The thickness of the vapor layer is much smaller than the drop radius ( $e/R < 0.02$ ), and increases with it. Two distinct regimes are observed, with a transition around the capillary length (2.5 mm for water at 100 °C). Although the range of observation is quite small (and cannot be made larger for big puddles, as shown earlier), scaling laws are observed, giving as successive exponents  $1.25 \pm 0.10$  and  $0.50 \pm 0.05$ .

In this stationary regime, the vapor film is supplied by the evaporation of the drop, but flows because of the drop weight. Both corresponding flow rates can be evaluated.

First, the heat from the plate is diffused across the vapor layer. We denote  $\Delta T$  as the difference between the plate temperature and the boiling temperature of the liquid. As stressed earlier, we checked that the water drop is indeed at 100 °C. We measured with a thermocouple the plate temperature as well, and thus determined  $\Delta T$  for each experiment.

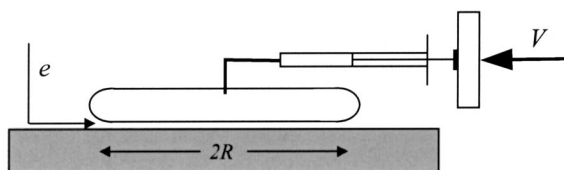


FIG. 6. Feeding a Leidenfrost drop at a constant rate provides a stationary state, where the drop radius  $R$  and the vapor film thickness  $e$  are observed to be constant.

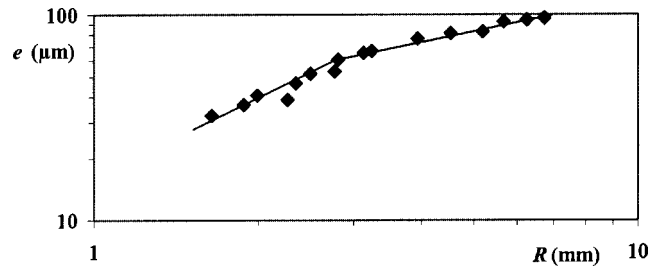


FIG. 7. Thickness of the vapor layer below a water drop (deposited on a duralumin plate at 300 °C and fed with water as sketched in Fig. 6), as a function of the drop radius  $R$ .  $R$  is varied by changing the feeding rate of the drop. The thin lines successively indicate the slopes 1.3 and 0.5. A kink is observed around the capillary length  $a = 2.5$  mm.

The heat  $Q$  brought to the liquid per unit time is proportional to the surface area  $\pi\lambda^2$  of the contact zone, to the thermal conductivity of the vapor  $\kappa$ , and to the temperature gradient  $\Delta T/e$ . Introducing the latent heat of evaporation  $L$ , we get for the rate of evaporation<sup>2</sup>

$$\frac{dm}{dt} = \frac{\kappa \Delta T}{L e} \pi \lambda^2. \tag{4}$$

Second, the drop weight induces a radial Poiseuille flow of vapor outside the layer.<sup>5</sup> The lubrication approximation can be used because of the small thickness of the vapor layer, as shown in Fig. 7. Thus, the flow rate scales as  $e^3 \Delta P / \eta \lambda$ , denoting as  $\Delta P$  the pressure imposed by the drop and  $\eta$  the gas viscosity. (Since  $\Delta P = \rho g h$  is of the order of 10 Pa, the associated density variations  $\delta\rho/\rho$  are of the order of  $10^{-4}$  and can be neglected.) Integrated over the contact, and written as a mass per unit time, it gives (in absolute value)

$$\frac{dm}{dt} = \rho_v \frac{2\pi e^3}{3\eta} \Delta P, \tag{5}$$

where  $\rho_v$  is the vapor density.

In a permanent regime, the mass of the vapor film remains constant. Thus, we can deduce from Eqs. (4) and (5) the film thickness. For puddles ( $R > a$ ), the contact and the drop radius are comparable ( $\lambda \sim R$ ) and the pressure acting on the film is  $2\rho g a$  [Eq. (2)]. This yields<sup>13–14</sup>

$$e = \left( \frac{3\kappa\Delta T\eta}{4L\rho_v\rho g a} \right)^{1/4} R^{1/2}. \tag{6}$$

For small drops ( $R < a$ ), we could use a similar argument: the contact is now given by Eq. (1) ( $\lambda \sim R^2/a$ ) and the pressure  $\Delta P$  acting on the film is the Laplace pressure, namely  $2\gamma/R$ . We would thus deduce that  $e$  varies as  $R^{5/4}$ . But for very small drops, we expect that the film plays a minor role in the evaporation process, since its surface area vanishes dramatically,<sup>9</sup> as  $R^4$  [as deduced from Eq. (1)]. Then, the temperature gradient should be of the order of  $\Delta T/R$ , and the evaporation process take place over the whole drop surface  $R^2$ . This gives, for the rate of evaporation,



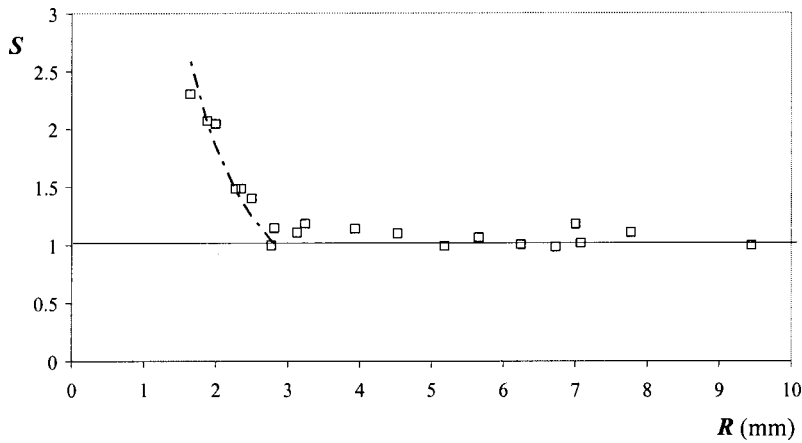


FIG. 8. Comparison between the measured rate of evaporation (given by the feeding rate of the drop, as sketched in Fig. 6) and the rate of evaporation in the film predicted by Eq. (4). We denote  $S$  as the ratio between both these rates, and plot it as a function of the drop radius  $R$ , for the same experimental conditions as in Fig. 7. For large drops ( $R > a$ ), we observe  $S = 1$ : the drop mainly evaporates via the film, while  $S$  is larger than 1 for smaller drops. Then, the data are fitted by the dotted line, which consider the evaporation on the whole surface, as described in Eq. (7).

$$\frac{dm}{dt} \sim \frac{\kappa \Delta T}{L R} R^2. \quad (7)$$

This rate is larger than the one given by Eq. (4) if  $R$  is smaller than  $(a^2 e)^{1/3}$ , i.e., practically for drops millimetric or less. The proportion of vapor which feeds the vapor layer scales as the surface area ratio  $\lambda^2/R^2$ . Using Eq. (5), the film thickness can finally be deduced:

$$e \sim \left( \frac{\kappa \Delta T \eta \rho g}{L \rho_v \gamma^2} \right)^{1/3} R^{4/3}. \quad (8)$$

On the whole, the film thickness is found to increase monotonically with the drop radius, but differently according to the drop size. The corresponding scaling laws are found to be in good agreement with the observations reported in Fig. 7.

These models depend crucially on the way the liquid is evaporated (by the surface or by the film). But the experiment described in Fig. 6 provides a direct measurement of the evaporation, which is equal to the (measured) feeding rate  $dm/dt$ , for a given drop size. We denote  $S$  as the ratio between this rate and the one predicted by Eq. (4), where all the parameters are known or measured: we take for  $\kappa$ ,  $\eta$ , and  $\rho$  their values at the average temperature in the vapor film (here 200 °C), which yields:  $\kappa = 0.032$  W/m/K,  $\eta = 1.63 \times 10^{-5}$  Pa s, and  $\rho = 0.5$  kg/m<sup>3</sup>. The value of the latent heat  $L$  at 100 °C is  $2.26 \times 10^6$  J/kg. In Fig. 8, the number  $S$  is plotted as a function of the drop radius.

It is found that above the capillary length (puddles), the drop indeed evaporates mainly via the vapor film ( $S = 1$ ), which justifies our hypothesis for establishing Eq. (6). But it is not the case for smaller drops: in Fig. 8, we observe  $S$  exceeds 1 for  $R$  smaller than  $a$ , and all the more since  $R$  is small. This deviation was expected from our discussion above, where we assumed that the evaporation of small drops was likely to occur on the whole surface, rather than mainly in the film. To be more precise, we drew in Fig. 8 with dotted lines the value of  $S$  expected if taking Eq. (7), instead of Eq. (4), for modeling the evaporation rate. The line nicely fit the data, with an adjustable parameter, which is the (unknown) coefficient in Eq. (7). The value provided by the fit for this numerical coefficient is found to be 118 [which reduces to 9.3 by taking into account the geometric factor  $4\pi$  in Eq. (7) for the nearly spherical drops representative in this

limit]. On the whole, we thus confirm with this experiment the existence of a global evaporation in the regime of small drops, which justifies the assumption used to derive Eq. (8).

#### IV. EVAPORATING DROPS

A Leidenfrost drop is usually not fed, and it is natural to follow its radius as a function of time.<sup>2,7,15</sup> Such a plot is displayed in Fig. 9, for two plate temperatures. Here the experiment is the following: a centimetric drop of water is first gently deposited on a hot duralumin plate, trapped within a copper annulus and filmed from above.

The drop radius regularly decreases, except at the end (when the drop becomes quasi-spherical). Then the variation becomes quicker, as reported earlier.<sup>4,6,9</sup> Note also that the evaporation is faster if increasing the plate temperature, which leads to a smaller lifetime, as already noted in Fig. 1. We saw in Sec. III that the radius and the film thickness are likely to be related to each other, which suggests that the film thickness could also vary with time. We measured the film thickness as the drop evaporates (Fig. 10), and found that it decreases as a function of time, confirming an earlier qualitative observation of Chandra.<sup>15</sup> The uncertainties in the measurements are due to the extreme mobility of the drop (which moves constantly and possibly vibrates). Moreover, both the contact zone and the film thickness become very small as the drop vanishes, which limits the diffracted intensity. As a matter of fact, only one or two maxima can then be obtained in the diffraction pattern.

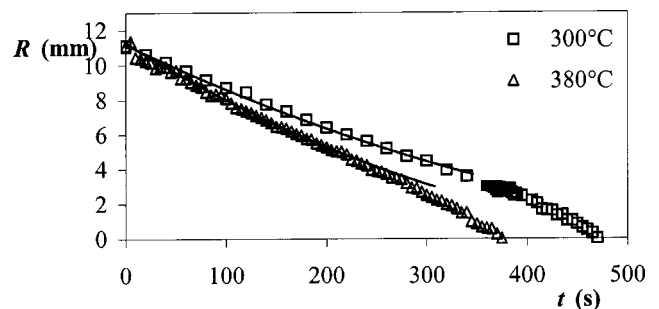


FIG. 9. Radius of a water drop deposited on a very hot duralumin plate (either 300 or 380 °C), as a function of time. The drop is filmed from above, and the lines show Eq. (9).

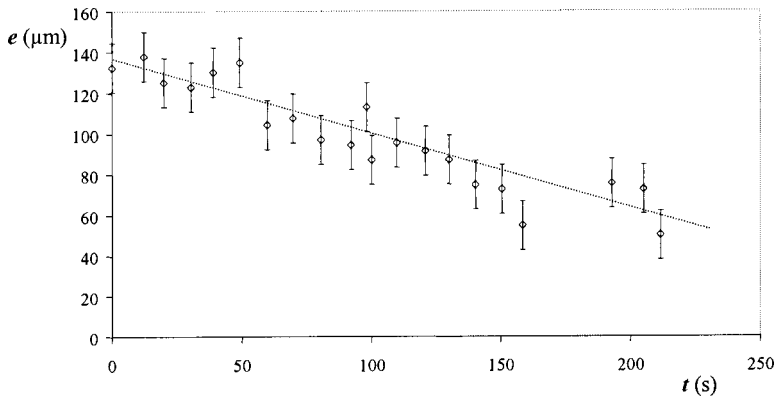


FIG. 10. Time dependence of the thickness of the vapor layer below a water drop of initial radius 1 cm deposited on a 350 °C duralumin plate. The data can be fitted by a straight line, as predicted by Eq. (11). If extrapolated to  $e=0$ , the line provides a lifetime  $\tau$  of  $400 \pm 50$  s.

But we observe quite clearly that the film thickness decreases with time. If extrapolated, the thickness is expected to reach zero at a time of the order (300–350 s) of the lifetime of a Leidenfrost drop at this temperature. Thus, as it evaporates, a Leidenfrost drop not only retracts but also slowly sinks. It disappears when both  $e$  and  $R$  cancel.

Our central assumption here is that the radius of the evaporating puddle and the thickness of the vapor film are related by Eq. (6) (quasistatic equilibrium). Then, we can deduce the time dependence of the radius from Eq. (5), considering that the evaporation is dominated by the vapor film. Denoting as  $R_0$  the radius at  $t=0$ , we find

$$R(t) = R_0 \left( 1 - \frac{t}{\tau} \right)^2 \quad (9)$$

with

$$\tau = 2 \left( \frac{4\rho a L}{\kappa \Delta T} \right)^{3/4} \left( \frac{3\eta}{\rho v g} \right)^{1/4} R_0^{1/2}. \quad (10)$$

Equation (9) fits quite well the data in Fig. 9, without any adjustable parameter, as long as the drop is a puddle ( $R > a$ ). It also provides a lifetime for these large drops, which is found to decrease as  $\Delta T^{-3/4}$ . Together with Eq. (6), Eq. (9) also allows us to predict the evolution law for the thickness of the vapor film. We find

$$e(t) = \left( \frac{3\kappa \Delta T \eta R_0^2}{4L\rho v g a} \right)^{1/4} \left( 1 - \frac{t}{\tau} \right). \quad (11)$$

Hence, we expect a linear variation for the film thickness, which should vanish as the drops collapse (for  $t = \tau$ ). Such a dependence agrees well with the observations reported in Fig. 10, where the slope is found to be  $-0.3 \pm 0.1 \mu\text{m/s}$ , close to the value deduced from Eq. (11) (without any adjustable parameter), which is  $de/dt = -0.21 \mu\text{m/s}$ . Besides, extrapolating to  $e=0$  the data in Fig. 10 provides a time  $\tau$  of  $400 \pm 50$  s, there again in good agreement with values extrapolated in Fig. 9, which give  $\tau = 400 \pm 30$  s.

For a smaller drop (or a large one at a longer time), it was stressed earlier that the evaporation occurs by the whole drop surface [Eq. (7)]. Integrating this equation for a sphere yields

$$R(t) = R_0 \left( 1 - \frac{t}{\tau} \right)^{1/2} \quad (12)$$

with

$$\tau \sim \frac{\rho L}{\kappa \Delta T} R_0^2. \quad (13)$$

Equation (12) implies an increase of the speed of retraction close to the time when the drop vanishes, which is in qualitative agreement with the observations. Equation (13) also provides the lifetime of a Leidenfrost droplet ( $R_0 < a$ ), which is found to be slightly more sensitive to temperature than a puddle, and much more dependent on the size.

## V. CONCLUSION

A Leidenfrost drop does not wet the hot solid on which it is deposited because it floats on a thin film of vapor. It thus exhibits the characteristics of nonwetting drops, i.e., a thickness of twice the capillary length  $a$  for large puddles, and a quasispherical shape for drops smaller than  $a$ , except a contact zone, whose size quickly vanishes as the drop gets smaller. Moreover, the vapor film can become unstable for very large drops, and thus the aspect ratio (diameter over thickness) was found to be limited by a value of order 4.

The thickness  $e$  of the vapor film was observed to depend on the drop radius  $R$ : it increases as  $R^{1/2}$  for puddles, and as  $R^{4/3}$  for drops smaller than  $a$ . Because of these relations, the drop does not only retract as it evaporates, but it also sinks. The lifetime of a Leidenfrost drop could finally be deduced from the evaporation kinetics. Again, the law for the lifetime depends on the size of the drop, compared with the capillary length. This is quite important to stress because most of the available data in the literature were obtained for millimetric drops, thus in the transition region.

Other remarkable features of Leidenfrost drops would deserve more detailed studies. We currently study the dynamics of formation of the film, which sets very rapidly. Comparing the time of formation of the film with the boiling time of the drop provides a criterion for the Leidenfrost temperature. We are also interested in the spontaneous vibration of these liquid balls (which deserve the name of Leidenfrost stars proposed by Mahadevan). Different details on their dynamics are also worth being reported, as is their very rapid motion due to their low friction, and their ability to bounce if thrown on the solids<sup>16</sup>—a major problem when trying to cool very hot steel plates, for example.

## ACKNOWLEDGMENTS

We thank Pascale Aussillous, Vance Bergeron, Frédéric Chevy, Élise Lorenceau, and L. Mahadevan for invaluable discussions and encouragement.

- <sup>1</sup>J. G. Leidenfrost, *De Aquae Communis Nonnullis Qualitatibus Tractatus* (Duisburg, 1756).
- <sup>2</sup>B. S. Gottfried, C. J. Lee, and K. J. Bell, "The Leidenfrost phenomenon: Film boiling of liquid droplets on a flat plate," *Int. J. Heat Mass Transf.* **9**, 1167 (1966).
- <sup>3</sup>K. J. Baumeister and F. F. Simon, "Leidenfrost temperature—Its correlation for liquid metals, cryogenes, hydrocarbons and water," *J. Heat Transfer* **95**, 166 (1973).
- <sup>4</sup>H. Bouasse, *Capillarité et Phénomènes Superficiels* (Delagrave, Paris, 1924).
- <sup>5</sup>C. T. Avedisian and J. Koplik, "Leidenfrost boiling of methanol droplets on hot porous/ceramic surfaces," *Int. J. Heat Mass Transf.* **30**, 379 (1987).
- <sup>6</sup>Y. M. Qiao and S. Chandra, "Experiments on adding a surfactant to water drops boiling on a hot surface," *Proc. R. Soc. London, Ser. A* **453**, 673 (1997).
- <sup>7</sup>C. T. Avedisian and M. Fatehi, "An experimental study of the Leidenfrost evaporation characteristics of emulsified liquid droplets," *Int. J. Heat Mass Transf.* **31**, 1587 (1988).
- <sup>8</sup>A. B. Wang, C. H. Lin, and C. C. Chen, "The critical temperature of dry impact for tiny droplet impinging on a heated surface," *Phys. Fluids* **12**, 1622 (2000).
- <sup>9</sup>L. Mahadevan and Y. Pomeau, "Rolling droplets," *Phys. Fluids* **11**, 2449 (1999).
- <sup>10</sup>P. Aussillous and D. Quéré, "Liquid marbles," *Nature (London)* **411**, 924 (2001).
- <sup>11</sup>G. I. Taylor, "The instability of liquid surfaces when accelerated in a direction perpendicular to their planes," *Proc. R. Soc. London, Ser. A* **201**, 192 (1950).
- <sup>12</sup>S. Chandrasekhar, *Hydrodynamic and Hydromagnetic Stability* (Dover, New York, 1981).
- <sup>13</sup>L. H. J. Wachters, H. Bonne, and H. J. van Nouhuis, "The heat transfer from a hot horizontal plate to sessile water drops in the spheroidal state," *Chem. Eng. Sci.* **21**, 923 (1966).
- <sup>14</sup>B. S. Gottfried and K. J. Bell, "Film boiling of spheroidal droplets," *I&EC Fundamentals* **5**, 561 (1966).
- <sup>15</sup>S. Chandra and S. D. Aziz, "Leidenfrost evaporation of liquid nitrogen droplets," *J. Heat Transfer* **115**, 999 (1994).
- <sup>16</sup>L. H. J. Wachters and N. A. J. Westerling, "The heat transfer from a hot wall to impinging water drops in the spheroidal state," *Chem. Eng. Sci.* **21**, 1047 (1966).